Finite Element Analysis and Experiments of Milli-Part Forming of Strip Bending Using Grain Element

T.W. Ku, D.J. Kim, and B.S. Kang

Abstract

Milli-structure components are classified as a component group whose size is between macro and micro scales, that is, about less than 20mm and larger than 1mm. The bending of these components of thin sheets has a typical phenomenon of bulk deformation because of the forming size. The recent trend towards miniaturization causes an increased demand for parts with very small dimensions. The conceptual miniature bending process enables the production of such parts with high productivity and accuracy. The stress values of the flow curve decrease with miniaturization, which means that, coarse grained materials show a higher resistance against deformation, when the grain size is in the range of the sheet thickness. In this paper, a new numerical approach is proposed to simulate intergranular milli-structure in forming by the finite element method. The grain element and grain boundary element are introduced to simulate the milli-structure of strip in the bending. The grain element is used to analyze the deformation of individual grain while the grain boundary element is for the investigation on the movement of the grain boundary. Also, the result of the finite element analysis is confirmed by a series of milli-sized forming experiments.

Key Words : Milli-structure, Grain Element, Grain Boundary Element, Finite Element Method, Strip Bending

1. Introduction

With the ongoing miniaturization in the field of small part manufacturing, as well as many other technical fields, there is a growing demand for the development of accurate forming process for thin sheet as a general trend towards higher integration and packaging densities[1,2].

Due to the trend of miniaturization the specific advantages of metal forming, especially the high productivity and the high material utilization, can not be exploited to the same extent in the field of milli-component production as in conventional metal forming[3,4].

Also, the milli-component has together with the microscopic properties, crystal plasticity and grain size etc., and macroscopic properties of conventional metal forming[5,6].

However, todays micro-forming is largely characterized by empirical process design, which

* Pusan National university

leads to a merely limited application of the specific advantages. In contrast to the conventional metal forming, the numerical simulation methods are hardly used for metal flow analysis or tool design in micro-forming[7]. The reason is that the simulation methods by definition are size independent; i.e. they cannot be applied straightway to micro-forming problems because of the size effect. One of the problems which are encountered in the development of such processes is the variation in product quality and in the magnitude of the process force of the blank holding force and punch loads. The occurrence of this problem is directly related to the ratio of grain size to sheet thickness. As the sheet thickness decreases to the same order of magnitude as the grain size, the mechanical properties of the individual grains will dominate the properties of the sheet. The problem can be solved by integrating the size effect into the models used in the simulation[8,9].

The main goal of this study is to provide fundamental information on the milli-structure rectangular deep drawing process, the corners of which can be counted as parts of micro-forming while whole of the forming characteristics show macro-forming. A systematic approach of the finite element method has been carried out for the design of the forming processes of milli-structure rectangular deep drawing. Although the finite element method provides valuable information on the deformation of polycrystals, it is impossible to simulate the motion of individual grains in the granular polycrystalline materials. To circumvent these difficulties a new approximate model is proposed. The idea is to represent the polycrystalline material by an aggregate of so-called grain elements that describe the plastic deformations of each individual grain[10]. Free grain boundary shearing and compression are accounted for by grain boundary elements, connecting the grains.

In the present study, formulations for describing the motion of grains and the interaction of grain boundary in granular polycrystalline materials are presented on the basis of the underlying micro-structure and physical mechanism.

The proposed method was applied to deep drawing as a strip bending process that sheet thickness was 0.4mm. The results of simulations and experiments were compared in view of the deformation of individual grain. The deformation area of the specimen was observed by a microscope facilitating the distribution and the deformation of grains.

2. Finite Element Model of Grain and Grain Boundary Element

A planar polycrystalline material is considered which consist of hexagonal grains. Each grain is represented by a special-purpose finite element, with the grain element to account for plastic deformation of individual grains. The grain elements are connected by grain boundary elements to account for shear deformation between grains. In the approach, each grain element can be regarded as a six node element that consists of two quadrilaterals shown in Fig.1(a). The constitutive description of the grain element is the viscoplastic, and the grain boundary element follows the modified viscoelastic behaviors.

2.1 Grain Element Formulation

The deforming body is composed of a rigid-viscoplastic material which obeys the von Mises yield criterion and its associated flow rule. In the variational approach, a stationary value is sought for a variational functional. The minimization of the functional produces a set of differential equations that is called Euler equations which are expected to be the same as the given boundary value problem. Thus, the function which minimizes that functional is also the solution of the boundary value problem. From the variational approach, the finite element governing equation can be obtained from the following functional[11]

$$\Pi = \int_{\Omega} \bar{\sigma}\, \bar{\varepsilon} d\Omega - \int_{T_{hi}} h_i u_i dT \tag{1}$$

The incompressibility constraint on admissible velocity fields may be removed by introducing a penalty constant, ***K*** and modifying the above equation (1). Then, the solution of the original boundary-value problem is obtained from the solution of dual variational problem, where the first order variation of the functional vanishes, where ***K*** a penalty constant, is a very large positive constant. $\delta \bar{\varepsilon}$ and $\delta \dot{\varepsilon}_V$ is the variation in strain rate derived from δu_i

$$\delta\Pi = \int_{\Omega} \bar{\sigma}\, \delta \bar{\varepsilon} d\Omega + K\int_{\Omega} \dot{\varepsilon}_V \delta \dot{\varepsilon}_V - \int_{T_{hi}} h_i \delta u_i dT \tag{2}$$

Equation (2) is the basic function of grain element behavior for the finite element discretization. This equation can be converted to nonlinear algebraic equations by utilizing the discretization procedure. The finite element discretization is performed on the element level with domain $\Omega^{(e)}$ and boundary $T^{(e)}$ for each element. The solution of the nonlinear simultaneous equations is obtained by direct iteration method and Newton-Raphson method.

2.2 Grain Boundary Element Formulation

To consider the size effect in the micro forming, the grain elements and grain boundary elements are used. The grains in the sheet metal are modeled by the grain elements which are connected by grain boundary elements[12]. Each grain element is regarded as a six-node element that consists of two quadrilaterals with each quadrilateral being built up of four-node element and the grain boundary element is as a four-node element as shown in Fig.1(a).

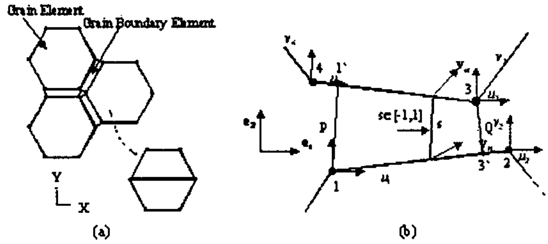

Fig.1 Schematic of grain element and grain boundary element

The mathematical relations for the grain boundary elements can be derived at each step during the incremental procedure, based in the current configuration of Fig.1(b). The grain boundary element is associated with the segment 1-3′ and 1′-3, where 1′ and 3′ are the orthogonal projections of 1 and 3 on the opposite grain element. A local coordinate s ∈ [-1,1] and a local set of base vectors (e_1, e_2) are connected to each midpoint. The compression rate α and shearing rate β at each node in grain boundary element are defined like,

$$\alpha = (\mathbf{v}_m - \mathbf{v}_n)\cdot \mathbf{e}_1 \tag{3}$$

$$\beta = (\mathbf{v}_m - \mathbf{v}_n)\cdot \mathbf{e}_2 \tag{4}$$

where V_m and V_n are the velocity vectors at the nodes of the adjacent grains. Upon discretization for finite element formulation, V_m and V_n are arranged as linear interpolations between the velocities in the grain nodes 1, 2 and 3, 4, respectively. Equation (3) and (4) are rewritten by using the nodal velocities.

$$\alpha=\frac{1}{2}(u_1-u_4)(1-s)e_1+\frac{1}{2}(u_2-u_3)(1+s)e_1 \quad (5)$$
$$+\frac{1}{2}(v_1-v_4)(1-s)e_2+\frac{1}{2}(v_1-v_3)(1+s)e_2$$

$$\beta=\frac{1}{2}(u_1-u_4)(1-s)e_2-\frac{1}{2}(u_2-u_3)(1+s)e_2 \quad (6)$$
$$+\frac{1}{2}(v_1-v_4)(1-s)e_1+\frac{1}{2}(v_1-v_3)(1+s)e_1$$

The mathematical description of the grain boundary element is nonlinear viscous-like constitutive equations which is quite different from the rigid-viscoplastic constitutive equations for the grain elements. For numerical convenience, the fictitious layer of linear elastic springs against compression and shearing[13]. The mathematical formulation of the grain boundary element is described by the following visco-elastic relationships,

$$\dot{\tau}=k_s(\alpha-\alpha_m) \quad (7)$$

$$\dot{\sigma}=k_n(\beta-\beta_m) \quad (8)$$

where k_s and k_n are the elastic stiffness of the shearing and compressing, α_m and β_m are small positive constant for numerical treatment, respectively.

From the variational approach, the governing equation of grain boundary element can be obtained from the following functional

$$\Pi_{GBE}=\int_\Omega[k_n(\alpha-\alpha_m)+k_s(\beta-\beta_m)]d\Omega \quad (9)$$

and the first order variation of the functional is written by following equation

$$\delta\Pi_{GBE}=\int_\Omega(k_n\alpha\delta\alpha+k_s\beta\delta\beta)d\Omega \quad (10)$$

Equation (10) also is converted to nonlinear algebraic equations by utilizing the discretization procedure. The solution of the equations is calculated simultaneous with equation (2).

3. Finite Element Simulations of Strip Bending Process

The product is a tiny rectangular vibrator case of cellular phones of which the manufacturing processes consist of five stages of blanking, drawing, sizing, piercing and trimming. The sheet material is SPCE, and tapping oil is used for lubrication with the friction constant of 0.12[14]. The dimensions of sheet are 30mm width and 0.4mm thickness. The deep drawing process is analyzed to observe the grain distribution before and after the drawing. In this study, the finite element analyses are assumed by plane-strain bending, which is shown in Fig.2 as a simulation model. The number of grain elements are 910, and of grain boundary elements 1132. The radii of the punch and die are 0.4mm. In this model, the size of grain element is 50 μm which is a large than the real average initial grain size 13.2 μm.

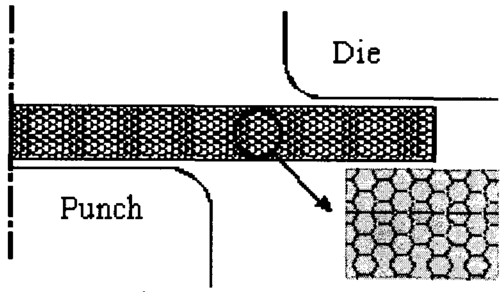

Fig.2 Initial mesh system of bending process

Figure 3 shows the result of simulation, the grain elements and the grain boundary elements are quite deformed at the corner and the wall in the deep drawn cup. Especially, the grain boundary elements in the wall are significantly distorted and difficult to see. This is due to the fact that the deformation mode in the corner and wall is strongly influenced by the shear deformation while the deformation at the bottom appears to be extension. Detailed view of bottom position is shown in Fig.4(a). The bottom deforms between the punch and the die. As shown in the figure, the deformation at the bottom is not severe but with small amount of extension.

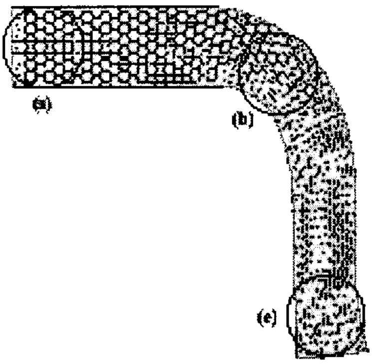

Fig.3 Deformation of grain elements and grain boundary elements

At the corner whose deformation is shown in Fig.4(b), the tensional deformation occurs along the longitudinal direction while the compressive one does through the thickness direction. Inside the corner bending, the grain boundary elements are severely distorted because of compression and the grain elements are also compressed. But, along the wall outside the corner bending, the grain boundary elements and grain elements become longer because of tension. These results are typical deformation in bending process.

In the wall(Fig.4(c)), the thickness is decreased since the grain boundary elements are quite distorted. The shear and tensile deformations are combined in the grain boundary elements. The grain elements are severely distorted with slight rotational movement because the shear deformation is more dominant and the sliding occurs between grains. These vivid graphical displaying can not be achieved by the conventional finite element analysis.

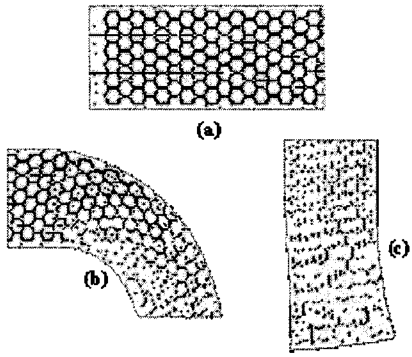

Fig.4 Detail views of deformation represented by grain elements and grain boundary elements (a) bottom (b) corner (c) wall

4. Rectangular Deep Drawing Experiments

For the confirmation of the previous numerical approach, a milli-structural part with plane-strain bending effect is formed by rectangular deep drawing. Some part of the experiment has been explained in the previous publication. However, for the completion of the paper, the summary is followed.

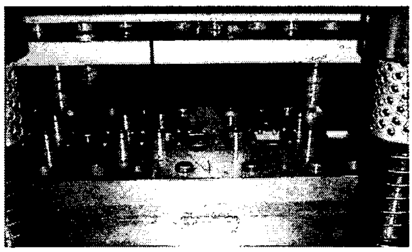

Fig.5 Progressive dies for the manufacturing of the milli-structure deep drawing part

Figure 5 shows the progressive dies to manufacture a milli-structure rectangular deep drawing part. The press is operated with the binder closed-loop force control, while the punch is under position control. Binder forces in the range of 250-350N and a constant punch stroke of 4mm were used for all tests

The dimensions and the final product of rectangular deep drawing are shown in Fig.6., and the final product of rectangular deep drawing in Fig.7.

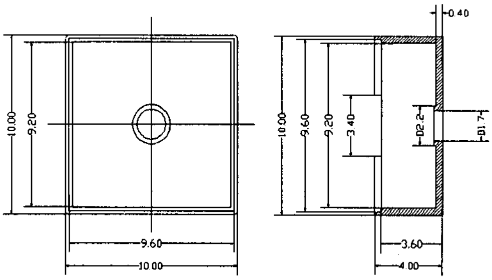

Fig.6 Final product geometry(unit:mm)

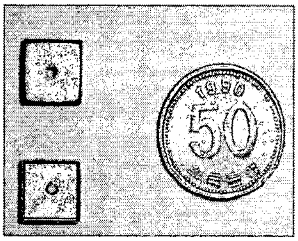

Fig.7 Final product of the milli-structure rectangular deep drawing part

The observations in view of micro-structure of the grain distribution and the change of grain size before and after milli-scaled part forming were made at the section A-A in Fig.8. Figure 8 is the sectioned configuration of the pre-treated specimen by using SEM.

Figure 9 shows the microphotograph of the grain distribution at the position B. The circularization and overlapping phenomena of the grains due to the compression force at the inside corner, in Fig.9(a), are noticed to be noteworthy. In contrast, the length extension phenomena of the grains because of the local tension force in the outside corner appears, which is shown in Fig.9(b).

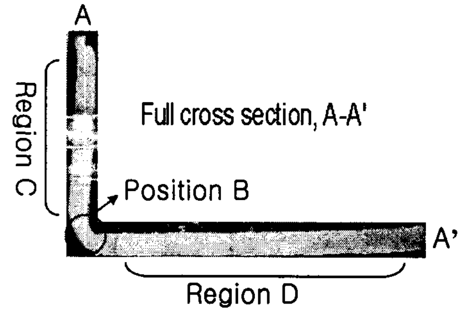

Fig.8 Sectioned configuration of the specimen

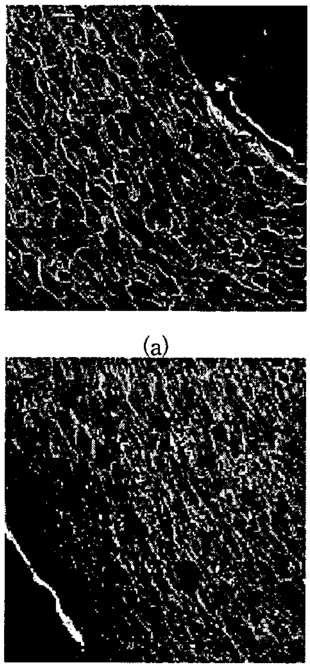

(a)

(b)

Fig.9 Microphotograph of the grain distribution at the corner B(×400)

In Fig.10, the microscopic figure shows the grain deformation of the side wall and the bottom, where the average grain size in the region C(side wall), and region D(bottom region) are about 29.87 μm, 14.65 μm, respectively. It is noticed that the grain structure of the region D appears to be almost the same as that of the initial blank, while the grain deformation of the region C shows severe distortion comparing with the initial blank which are same results of finite element simulation of Fig.4.

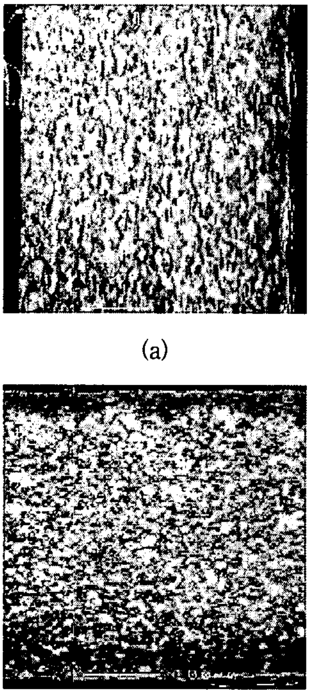

(a)

(b)

Fig.10
Grain configuration at the wall(a) and the bottom(b) respectively (×400)

Compared with the initial blank grain size of 13.20 μm, the grain size after deep drawing process in Fig.10(b) increases slightly to 14.65 μm, indicating that small plastic deformation is introduced at the region D. However, the grain size at the region C after deep drawing process in Fig.10(a) increases obviously to 29.87 μm, which is more or less two times larger than the initial grain size of the blank. This phenomenon attributes to the large elongation occurred in this area. Simultaneously, the effect of friction condition applied to the region C is much stronger than to the region D. It should be noted that the grain deformation in experiment is similar to the result from the new numerical approach using grain and grain boundary elements, even though there is slight differences in the grain sizes between experiment and numerical approach.

4. Concluding Remarks

A new numerical approach is proposed for the analysis of intergranular micro-structure by the finite element method, in which the grain and grain boundary element are introduced. The grain element is used to analyze the deformation of individual grain while the grain boundary element is for the investigation on the sliding and the extension between elements.

In the experimental confirmation by the deep drawing in view of the plane-strain bending, the deformation of the bottom is not so severe both in the experiment and the numerical simulation. At the bended corner, the size of grain element inside the bended corner becomes smaller after forming due to compressive deformation mode while that outside the bended corner does larger due to extensional deformation mode. These trend of deformation is shown both in the experiment and the simulation with good agreement in view of the deformational appearance.

Since the deformation trend and the prediction of the thickness change by the numerical analysis is almost the same as the experimental result, it is expected that the proposed numerical approach can be applied to miniature forming of milli-sized components.

Acknowledgements

This work has been funded partially by the ERC for Net-Shape and Die Manufacturing, Pusan National University, Korea. Also, the last author would like to acknowledge the support of the research program, Milli-structure manufacturing technology by Ministry of Commerce, Industry and Energy of Korea, 2000.

REFERENCES

(1) M., Geiger, F., Vollertsen and R., Kals, 1996, "Fundamentals on the Manufacturing of Sheet Metal Microparts", Annals of the CIRP, Vol.45, pp.227

(2) A., Tseng, 1990, "Material Characterization and Finite Element Simulation for Forming Miniature Parts", Finite Element Annal. Des., Vol.6, pp.251

(3) S., Miyazaki, H., Fujita and K., Hiraoka, 1979, "Effect of Specimen Size on the Flow Stress of Polycristalline Cu-Al. Alloy", Scripta Met., Vol.6, pp.447

(4) Y., Marumo, H., Siki and A., Onoue, 2001, "Effects of Lap Sheets on the Improvement of the Formability of Metal Foil", J. of Materials Processing Technology, Vol.113, pp.627

(5) T., Jimma and T., Adachi, 1993, "Recent Trends in Precise Press-Working of Electronic Components", Proc. of the 4th Int. Con. on Technology of Plasticity, pp.1547

(6) M.N., Yoshito, 1979, "Influence of Microstructural Inhomogeneity on the Formability and Fracture of a Carbon Steel", Transaction of the ASME, Vol.101, pp.18

(7) A. Messner, U. Engel, R. Kals and F. Vollertsen, 1994, "Size effect in the FE-simulation of micro-forming processes", J. of Materials Processing Technology, Vol.45, pp.371.

(8) L.V., Raulea, A.M., Goijaerts, L.E., Govaert and F.P.T., Baaijens, 2001, "Size Effects in the Processing of Thin Metal Sheets", J. of Materials Processing Technology, Vol.115, pp.44

(9) R., Kals, F., Vollersten and M., Geiger, 1996, "Scaling Effects in Sheet Metal Forming", Proc. of the Int. Con. on Sheet Metal, pp.65

(10) T.A., Kals and R., Eckstein, 2000, "Miniaturization in Sheet Metal Forming Working", J. of Materials Processing Technology, Vol.103, pp.95

(11) M.F., Ashby, 1972, "Boundary Defects and Automic Aspects of Boundary Sliding and Diffusional Sreep", Surface Science, Vol.31, pp.498

(12) S., Kobayashi, S.I., Oh and T., Altan, 1989, "Metal Forming and the Finite Element Method", Oxford University Press

(13) P., Onck and E., Giessen, 1997, "Microstructurally-based Modeling of Intergranular Creep Fracture using Grain Elements", Mechanics and Materials, Vol.26, pp.109

(14) T.W., Ku and S.M., Hwang and B.S., Kang, 2001, "Milli-Component Forming of Rectangular Cup Drawing", J. of Materials Processing Technology, Vol.113, pp.749